Temperature-Dependent Relaxation of the Crystal-Amorphous Interphase in Poly(ether ether ketone)

Pengtao Huo and Peggy Cebe*

Department of Materials Science and Engineering, Massachusetts Institute of Technology, Cambridge, Massachusetts 02139

Received June 3, 1991; Revised Manuscript Received August 19, 1991

ABSTRACT: The temperature dependence of molecular mobility in the amorphous phase of poly(ether ether ketone), PEEK, was characterized by the dielectric relaxation intensity, $\Delta\epsilon = \epsilon_s - \epsilon_\infty$, at temperatures above the glass transition to determine the contribution that the crystal/amorphous interphase material makes to the relaxation process. Relaxation intensity is shown to be structure sensitive above T_g. For amorphous PEEK, $\Delta\epsilon$ initially decreases as temperature increases, then shows the opposite trend as the material crystallizes above T_g. For all semicrystalline PEEK, $\Delta\epsilon$ increases with temperature. The ratio of semicrystalline intensity to amorphous intensity determines the total fraction of dipoles which are already relaxed at a given temperature. Results indicate that the rigid amorphous phase in PEEK is not rigid at all temperatures but relaxes between the glass transition of the mobile amorphous phase and the melting point of the crystalline phase. The amount of crystal/amorphous interphase material joining the relaxation process increases as the temperature increases.

1. Introduction

Many semicrystalline polymers exhibit a morphology that can be described as consisting of lamellar crystals, amorphous material, and an intermediate region associated with the crystal/amorphous interphase.[1-8] Interphase regions are well known to exist in semiflexible chain polymers. Although a large fraction of the amorphous chains may be considered to be located in the interphase [see, for example, ref 8], all the amorphous chains in these polymers eventually attain the mobility level of the liquid-like state as temperature is increased above the glass transition temperature. However, in certain polymers with less flexible structures, it has been shown that a portion of the amorphous phase remains rigid above T_g.[9-15] This portion has been called the "rigid amorphous phase",[9-15] RAP, and is the amorphous fraction that does not become liquid-like above T_g as measured from the heat capacity increment.[9-15] To examine the molecular mobility of the interphase region, we have used dielectric relaxation spectroscopy. This approach has been used in our group previously to study poly(phenylene sulfide), PPS,[16,17] and by other researchers studying poly(ethylene terephthalate), PET.[18,19]

Our previous study of PPS[16,17] provided the first information for that polymer about the temperature-dependent relaxation of interphase chains which are constrained and exhibit decreased molecular mobility. In that work, we showed that the dipolar relaxation intensity associated with the glass-transition relaxation is an extremely sensitive indicator of mobility of the rigid amorphous-phase fraction. Dielectric relaxation can be used to quantify the total amount of the amorphous phase which is already relaxed at a given temperature. Using dielectric relaxation, we were able to show that the rigid amorphous phase relaxes in the temperature interval between T_g and the melting point.

In PPS, because of our new heat of fusion data,[17,20] the amount of rigid amorphous phase is calculated to be much larger than that reported previously,[15] ranging in our study from 0.33 to 0.42 for cold crystallized polymer.[17,20] We wanted to test our approach on a polymer with a much smaller amount of rigid amorphous phase but a comparable degree of crystallinity. For this study we chose PEEK in which the rigid amorphous-phase content ranges from 0.24 to 0.32. In both PEEK and PPS, the degree of crystallinity was in the range 0.28 to 0.37. Thus, a major difference in these two polymers will be the relative amounts of mobile amorphous and rigid amorphous dipoles.

2. Theoretical Section

Here we review the essential aspects of dielectric analysis used in this work. The complex dielectric function, $\hat{\epsilon} = \epsilon' - i\epsilon''$, can be written according to the Havriliak and Negami formulation of the Debye equations as[21]

$$\hat{\epsilon} = \epsilon_\infty + \frac{(\epsilon_s - \epsilon_\infty)}{(1 + (i\omega\tau)^{a_1})^{a_2}} \tag{1}$$

Parameters a_1 and a_2 ($0 < a_i < 1$) describe the degree of departure from the Debye equations[22] for which $a_1 = a_2 = 1$. ϵ_∞ and ϵ_s are the high and low frequency limiting values of ϵ', ω is the angular frequency, and τ is the central relaxation time for the process of interest. Here, we assume that we have a single relaxation process which is characterized by a distribution in the relaxation time.

The strength of a relaxation process is called the dielectric relaxation intensity, $\Delta\epsilon(T)$, and is proportional to the number of dipoles per unit volume which are capable of absorbing energy from the applied field at a given temperature.[22] The relaxation intensity can be found from the following relationship:

$$\Delta\epsilon(T) = \epsilon(T)_s - \epsilon(T)_\infty \tag{2}$$

In a manner analogous to heat capacity,[16,18,19] we define a normalized dielectric increment to represent the fraction of mobile amorphous dipoles which participate in the relaxation process at temperature $T > T_g$. We define a parameter $\beta(T)$ for the semicrystalline polymer as

$$\beta(T) = \frac{\Delta\epsilon(T)^{sc}}{\Delta\epsilon(T)^{a}} \tag{3}$$

where the superscripts sc and a refer to the semicrystalline and amorphous polymer, respectively. $\beta(T)$ is the relaxation intensity of the amorphous phase in the semicrystalline polymer normalized to the relaxation intensity of the 100% amorphous polymer. Using eq 2, we write

0024-9297/92/2225-0902$03.00/0

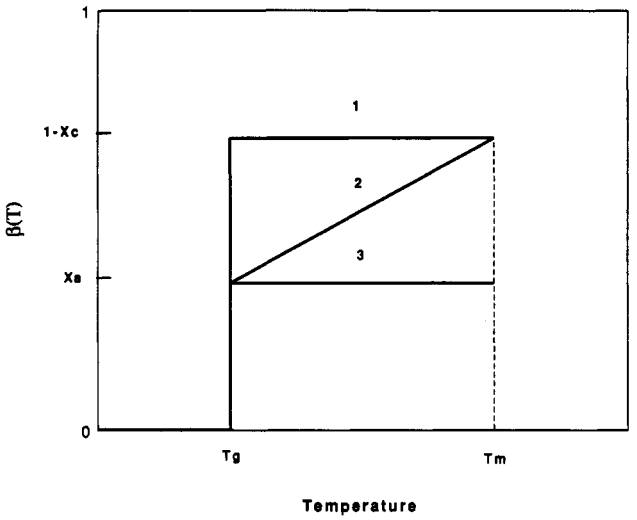

Figure 1. Idealized schematic plot of the total amount of amorphous phase relaxed, $\beta(T)$, as a function of temperature.

the dielectric increments in the numerator and denominator of eq 3 explicitly as

$$\beta(T) = \frac{\epsilon(T)_g^{sc} - \epsilon(T)_\infty^{sc}}{\epsilon(T)_g^{a} - \epsilon(T)_\infty^{a}} \quad (4)$$

$\beta(T)$ is the dielectric analogue of the heat capacity increment and represents the total fraction of dipoles participating in this relaxation process.[16,18,19] A sketch of $\beta(T)$ is shown in Figure 1 for three idealized cases which are described below.

The definition of $\beta(T)$ in eq 3 is valid above T_g. Below T_g, the limiting value of $\beta(T)$ should be zero since, for a single process representing the glass transition, there is no large-scale segmental movement. Above T_g but below T_m, three different cases are identified and are shown in Figure 1. The first case is the simplest two-phase model, which consists of crystal and amorphous phases. The amount of crystal phase is χ_c, and the amount of amorphous phase is $1 - \chi_c$. Either there is no distinct third phase (very small interphase component) or, if there is a significant interphase, it has the same thermal properties, such as heat capacity, as the amorphous phase. For a material exhibiting this two-phase behavior, $\beta(T) = 1 - \chi_c$ above T_g as shown in Figure 1, curve 1. This indicates that all of the amorphous phase becomes rubbery, or relaxed, at T_g and no additional material relaxes between T_g and T_m. The value of $\beta(T)$ at T_g is equal to the total amount of amorphous phase. Polymers such as polyethylene[9,10] and PTFE[11] are identified to be in this category according to heat capacity measurements.

The second possibility is that the polymer consists of three distinct phases: crystal (χ_c), mobile amorphous (χ_a), and rigid amorphous phases ($1 - \chi_c - \chi_a$). The latter is located in the crystal/amorphous interphase region. It has been shown to have a different thermal property (heat capacity) compared to the mobile amorphous phase.[9-15] It is still in the solid state at T_g of the mobile amorphous phase and does not exhibit its own distinct T_g and therefore has the same heat capacity as glassy polymer at T_g. As shown in Figure 1, curve 2, at T_g a polymer with this behavior has a step in $\beta(T)$ at T_g, attaining a value, χ_a, that is the same as the amount of mobile amorphous phase but less than the total amount of amorphous-phase material, $1 - \chi_c$. Above T_g, this material can become relaxed little by little as the temperature is increased from T_g up to T_m. Finally, all the interphase material becomes relaxed and $\beta(T) = 1 - \chi_c$. This category includes polymers such as PPS[16,17] and PET.[18,19,37]

The third model also assumes the existence of three phases, including an interphase. However, as shown in Figure 1, curve 3, the interphase material is not contributing to $\beta(T)$ above T_g. At T_g, only the mobile amorphous phase contributes to $\beta(T)$. $\beta(T)$ increases from zero below T_g to a value equal to χ_a, the mobile amorphous fraction. Then, there is no further change in $\beta(T)$ with increasing temperature. The interphase material is extremely "rigid" such that it does not relax in the temperature range between T_g and T_m. A polymer such as poly(oxymethylene)[13] is one of the examples. Originally, it was suggested by Cheng et al.[14,15] that PPS and PEEK may belong to this category, with a rigid amorphous fraction that does not relax until crystals had melted. We have since demonstrated that the rigid amorphous phase in PPS relaxes in the manner suggested by curve 2.[16,17] Here, we examine PEEK to determine the relaxation behavior of its rigid amorphous phase which is much smaller, relative to the mobile amorphous fraction, than it is in PPS.

3. Experimental Section

PEEK material (450G) was obtained in pellet form from ICI Americas, Inc. An amorphous film was made by compression molding the pellets at 400 °C for 2 min between ferrotype plates and then quenching in ice water. The quenched films were completely amorphous, showing a typical amorphous wide angle X-ray scattering pattern[23-25] and having a density of 1.264 g/cc.[23,26] Semicrystalline films were made by heating the amorphous films inside a Mettler FP80 hot stage, in an inert gas environment. The quenched amorphous film was heated from room temperature to the cold crystallization temperature and held there for 1 h.

The thermal characteristics of all the films are listed in Table I. Degree of crystallinity, χ_c, was determined from DSC, using 31.12 cal/g as the heat of fusion of 100% crystalline PEEK.[23] The mobile, or liquid-like, amorphous fraction, χ_a, refers to the portion of the amorphous phase contributing to the heat capacity increment at T_g. In general, at any temperature, we can define a heat capacity increment, $\gamma(T)$, as

$$\gamma(T) = \frac{Cp(T)_{liquid}^{sc} - Cp(T)_{solid}^{sc}}{Cp(T)_{liquid}^{a} - Cp(T)_{solid}^{a}} \quad (5)$$

where the superscripts have the same meaning as before. We evaluate $\gamma(T)$ for $T = T_g$ by linearly extrapolating the solid heat capacity from below T_g and liquid heat capacity from above T_g. This extrapolation allows us to calculate $\gamma(T_g)$, which gives the total of mobile relaxing units, i.e., χ_a, the fraction of the amorphous phase in the semicrystalline sample which is relaxing at T_g. The rigid amorphous-phase fraction χ_{RAP} is found from $\chi_{RAP} = 1 - \chi_a - \chi_c$.[9-15]

The glass transition temperature and heat capacity step at T_g were measured using a Perkin Elmer DSC-4 instrument. The glass transition temperature listed in the fifth column of Table I was obtained at 20 °C/min scan rate. This we will call the calorimetric T_g. Indium was used as the temperature calibrator, and a sapphire standard was used for heat capacity. The last column of the table lists the glass transition temperature determined from the position of the dielectric loss peak maximum at a frequency of 10 kHz, which we will call dielectric T_g.

Dielectric relaxation experiments were performed using a Hewlett Packard impedance analyzer. All films had a layer of gold evaporated on both surfaces to serve as electrodes. The sample thickness ranged from 50–80 μm, depending upon the thermal treatment. The gold-coated films were placed between polished rigid electrodes and placed inside the hot stage. The measurement was taken as a function of temperature in a stepwise manner. On average, the temperature increased at a rate of about 2 °C/min. The parallel capacitance, C, and loss factor, $\tan\delta$, of the samples were measured over a frequency range from 1000 Hz to 1 MHz, from 30 to 260 °C. The dielectric constant and loss were obtained from the measured data in the manner described previously in our investigation of PPS.[16]

Table I
Thermal Properties of PEEK: Crystalline-, Amorphous-, and Rigid Amorphous-Phase Fractions and Glass Transition Temperatures

sample T_c (°C)	χ_c (±0.01)	χ_a (±0.01)	χ_{RAP} (±0.02)	T_g (°C)[a] (±0.3 °C)	T_g (°C)[b] (±0.3 °C)
quenched	0.00	1.00	0.00	145.1	164.0
180	0.28	0.40	0.32	159.1	179.0
200	0.29	0.41	0.30	158.5	178.5
220	0.31	0.41	0.28	158.0	178.0
240	0.33	0.40	0.27	157.6	177.7
260	0.34	0.40	0.26	156.8	176.3
280	0.35	0.40	0.25	155.7	175.2
300	0.36	0.40	0.24	154.8	174.2

[a] Measured by using DSC at scan rate of 20 °C/min. [b] Measured by using dielectric loss maximum at 10 kHz.

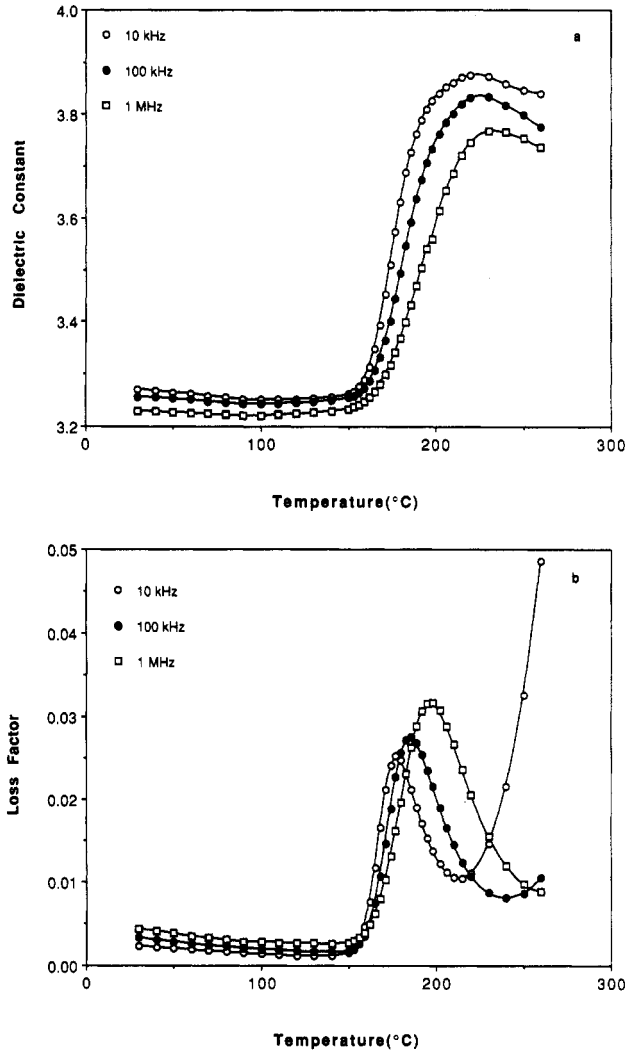

Figure 2. (a) Dielectric constant (ϵ') and (b) loss factor (tan δ) as a function of temperature for PEEK cold crystallized at T_c = 200 °C.

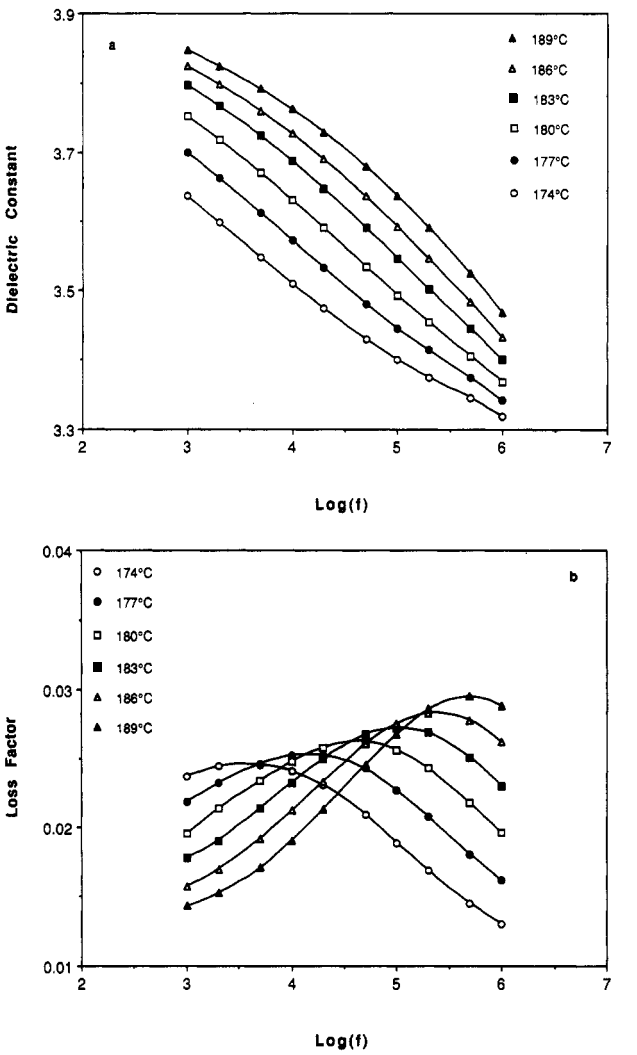

Figure 3. (a) Dielectric constant (ϵ') and (b) loss factor (tan δ) as a function of log (frequency) for PEEK cold crystallized at T_c = 200 °C.

4. Results and Discussion

4.1. Temperature- and Frequency-Dependent Dielectric Response. Dielectric relaxation results in the temperature range from 30 to 260 °C are shown in Figure 2 for the semicrystalline PEEK sample crystallized at 200 °C. The value of ϵ' is nearly constant prior to the relaxation and then increases sharply. The high-temperature value of ϵ' was observed to decrease slightly above 225 °C. The loss factor, tan δ, in Figure 2b shows the usual shape, reaching a maximum whose peak position shifts to higher temperature and whose peak maximum and width increase with increasing frequency. At the lower frequency, we see an upturn in the loss factor at high temperature, a result of increased ionic conductivity.

We see no evidence for a higher temperature relaxation process due to crystals, over the temperature range we studied. Crystal relaxation is often indicated by a peak or shoulder on the high-temperature side of the amorphous glass transition relaxation, as it is for polyethylene.[27] The steep upturn to very high intensity in the loss factor shown in Figure 2b is the result of ionic conduction. To avoid any possible conflict with high-temperature processes, in section 4.3 we have analyzed the relaxation intensity at temperatures below 200 °C.

A relaxation map of the cold crystallized PEEK is shown in Figure 3, parts a and b, for all the frequencies studied. ϵ' is shown as a function of log (f) for a series of temperatures in the vicinity of the glass transition relaxation process. In the temperature range from 174 to 189 °C, ϵ' decreases as frequency increases for a fixed temperature,

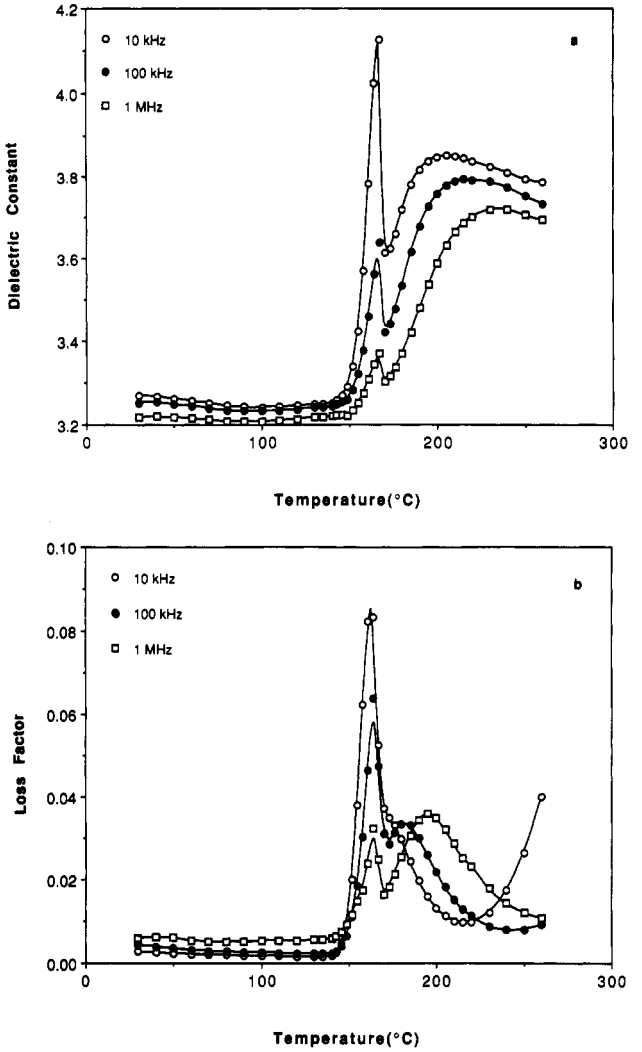

Figure 4. (a) Dielectric constant (ϵ') and (b) loss factor (tan δ) as a function of temperature for amorphous PEEK.

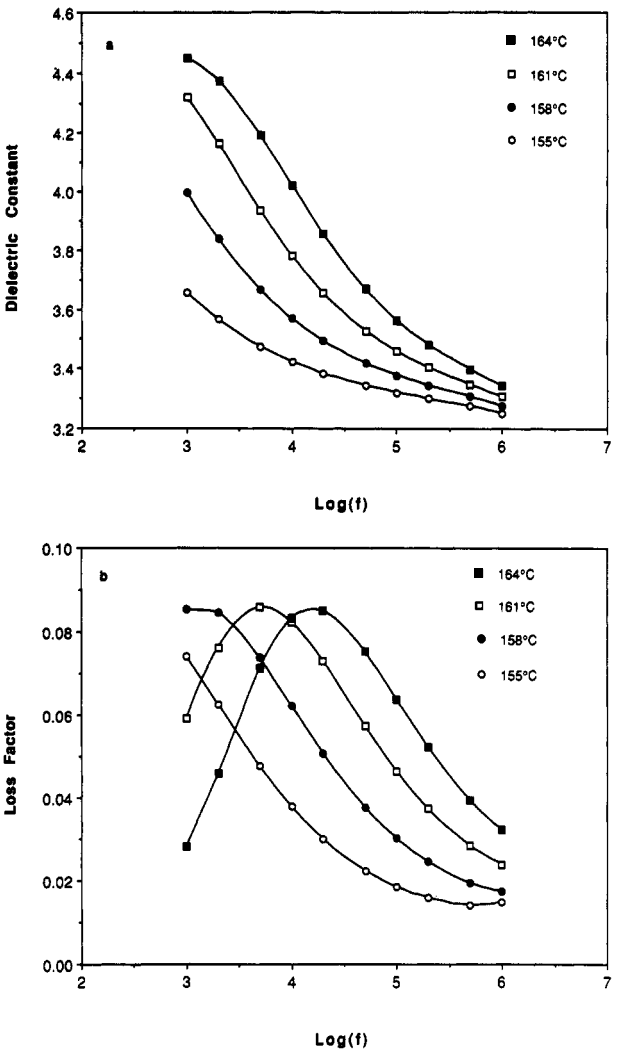

Figure 5. (a) Dielectric constant (ϵ') and (b) loss factor (tan δ) as a function of log (frequency) for amorphous PEEK.

and at a fixed frequency, ϵ' decreases with decreasing temperature. The tan δ results, shown in Figure 3, part b, indicate a shift in the frequency of the peak maximum to higher frequency as the temperature increases.

ϵ' and tan δ for quenched amorphous film are shown in Figure 4, parts a and b, for several frequencies. The glass transition relaxation begins at around 150 °C and ϵ' increases strongly to a maximum at about 160 °C. Rapid crystallization of the amorphous film above 164 °C results in a sudden decrease in ϵ'. There is an extra difficulty in converting the raw data (parallel capacitance) to ϵ' since the film thickness changes slightly during crystallization. From the known densities of the crystalline and amorphous phases, we calculated that the maximum change in thickness is expected to be about 2–3%, assuming that the final crystallinity is about 20%. This affects only the dielectric constant of amorphous PEEK (not tan δ) above 164 °C. When a precise quantitative value of dielectric constant is required, for example, when we measured the crystallization kinetics of PPS,[16] we used an analytical method to calculate the effect of changing film thickness. Readers interested in this approach should see the description in our previous work.[16]

The loss factor, shown in Figure 4, part b, is similarly affected by the crystallization. First, the amorphous film undergoes its glass transition relaxation and tan δ shows a strong maximum, which shifts slightly to higher temperature with increasing frequency. tan δ then decreases sharply due to crystallization and an additional relaxation is seen at higher temperature (around 195 °C for 10^6 Hz). The second peak is due to relaxation of the now-crystalline sample whose amorphous portion becomes constrained by the existence of crystals and therefore has a higher glass transition temperature. The shape and position of the second maximum is very close to that seen in Figure 2, part b, at the same frequency in the film cold crystallized at 200 °C.

The relaxation maps of the amorphous PEEK are shown in Figure 5, parts a and b, for all frequencies studied. The range of temperatures shown spans the glass transition region but stops before crystallization occurs. At fixed temperature, ϵ' decreases with increasing frequency, as in the semicrystalline PEEK. At fixed frequency, ϵ' decreases with decreasing temperature. The loss factor, shown in Figure 5, part b, indicates a shift in the loss peak maximum frequency to higher frequency with increasing temperature.

Dielectric relaxations in PEEK have been reported for amorphous and semicrystalline material.[28-30] Goodwin and Hay[28] present the dielectric loss factor over the temperature range 120–200 °C at one frequency, 10 kHz. Their data is for a material crystallized at 200 °C with degree of crystallinity of 25%, which is comparable to our PEEK sample shown in Figure 2. Our loss factor magnitude for the semicrystalline sample is larger by a factor of 2.5 compared to that reported by Goodwin and Hay. Even in our PEEK material which is 36% crystalline (cold crystallized at 300 °C), we never observed a loss peak

maximum as low as that reported by Goodwin and Hay. On the other hand, the loss factors for amorphous PEEK and for the now-crystallized amorphous material, shown in Figure 4, part b, are comparable to those of Goodwin and Hay. We are unable to compare our loss factor results to those of D'Amore et al.[29] because the loss factor presented by these authors had no units on the vertical axis.

In comparing the dielectric constant results, the only available data are those of D'Amore et al.[29] at 10 kHz. These authors report that the low-temperature (25 °C < T < 100 °C) dielectric constant of the amorphous PEEK film is very close to unity (implying that PEEK is about comparable to free space) and greatly differs from the semicrystalline film at the same temperature. We find instead that the amorphous and semicrystalline PEEK dielectric constants below 150 °C at 10 kHz are identical within experimental error and have the value of 3.26 relative to the permittivity of free space. Thus, our results indicate that the permittivity of PEEK below the glass transition temperature is dominated by local motions which appear to be insensitive to the degree of crystallinity. This dielectric result is supported by the mechanical relaxation data on storage modulus over the same temperature range,[31-36] though many of these studies were concerned primarily with effects of irradiation[31-33] or cross-linking[34,35] and not solely with degree of crystallinity.

4.2. Thermal Properties. Considering the relaxation maps of loss factor vs log (f), shown in Figures 3, part b, and 5, part b, these data allow the determination of activation energy for the glass transition relaxation process. Assuming that the relaxation process can be modeled by an Arrhenius temperature dependence,[22] the shift in the frequency of the loss peak maximum is plotted in Figure 6 as a function of reciprocal of the measurement temperature for amorphous PEEK and one representative semicrystalline PEEK sample. Limited data are available for the amorphous sample because of the rapid crystallization above the glass transition temperature. The data in Figure 6 were fit to a straight line whose slope is the apparent activation energy parameter for the glass transition relaxation process. For this relaxation process the activation energy, in general, will not be constant. For the limited range of frequencies accessible here, the apparent activation energies are

$$E_A(\text{amorphous}) = 780 \text{ kJ/mol}$$

$$E_A(T_c = 200\ ^\circ\text{C}) = 560 \text{ kJ/mol}$$

The apparent activation energies of other cold crystallized PEEK we studied are very close to 560 kJ/mol with variation in the range of ±20 kJ/mol.

The thermal transition behavior of PEEK has been studied extensively by our group[25,26,38] and others.[14,23,24,39-46] PEEK can be quenched directly from the melt into the glassy amorphous state.[23,26] When the material is then heated above its glass transition temperature, it undergoes cold crystallization from a state of low mobility. The glass transition temperature of 100% amorphous PEEK is 145 °C, as seen in Table I, and this agrees with previous reports for the commercial pellet-grade material.[23] However, when PEEK is cold crystallized, the glass transition temperature increases significantly as a result of the geometrical constraints of crystals on the amorphous phase.[26] In Table I we see that both calorimetric T_g and dielectric T_g shift up by 15 °C in PEEK cold crystallized at 180 °C. Dielectric T_g is always about 20 °C higher than calorimetric T_g, because of the difference in the effective frequencies in the dielectric experiment, compared to the DSC scan rate.[47]

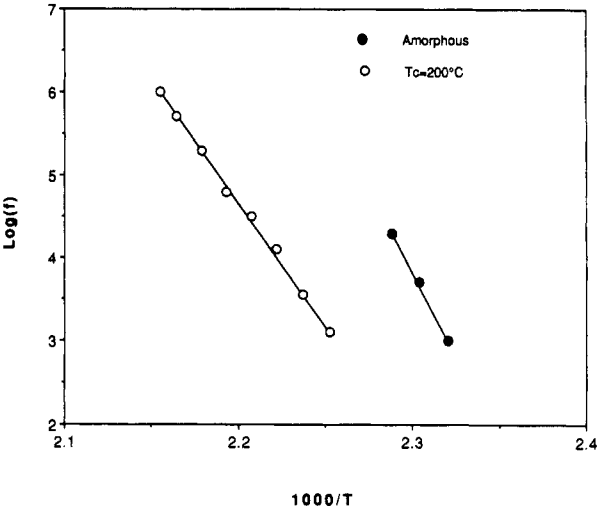

Figure 6. Log (frequency of the loss peak maximum) vs reciprocal temperature for amorphous and semicrystalline PEEK.

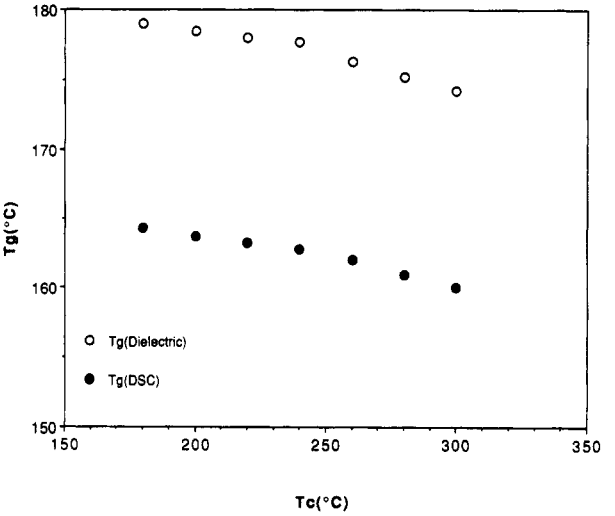

Figure 7. Glass transition temperature (T_g) as a function of crystallization temperature (T_c) for cold-crystallized PEEK: (●) measured by using DSC at scan rate of 20 °C/min; (○) measured by using dielectric loss maximum at 10 kHz.

In Figure 7, we present dielectric T_g and calorimetric T_g as functions of the crystallization temperature. Both measures of T_g show a systematic decrease as the crystallization temperature increases, in agreement with previous studies on cold crystallization of PPS.[14,16] As the cold crystallization temperature increases, the glass transition temperature of PEEK decreases in spite of the formation of additional crystals at the higher crystallization temperature.[25] The resultant decrease in the glass transition temperature may be attributed to relaxation of constraints on the amorphous phase, perhaps as a result of changes in the degree of entanglement of chains located at the crystal/amorphous interphase. In reality, all cold crystallizations listed in Table I must be considered as annealing of crystals formed at lower temperature. The reason is that all the crystallization temperatures are higher than the temperature of the maximum in the linear growth rate curve for PEEK.[23] Heating PEEK through the temperature of the maximum growth rate results in the formation of a population of imperfect crystals which continue to be perfected (annealed) at the crystallization temperature. It is not possible to heat PEEK sufficiently rapidly for the sample to equilibrate at the isothermal crystallization temperature before crystals have formed. The decrease in the glass transition temperature coincides with a decrease in the rigid amorphous phase content.

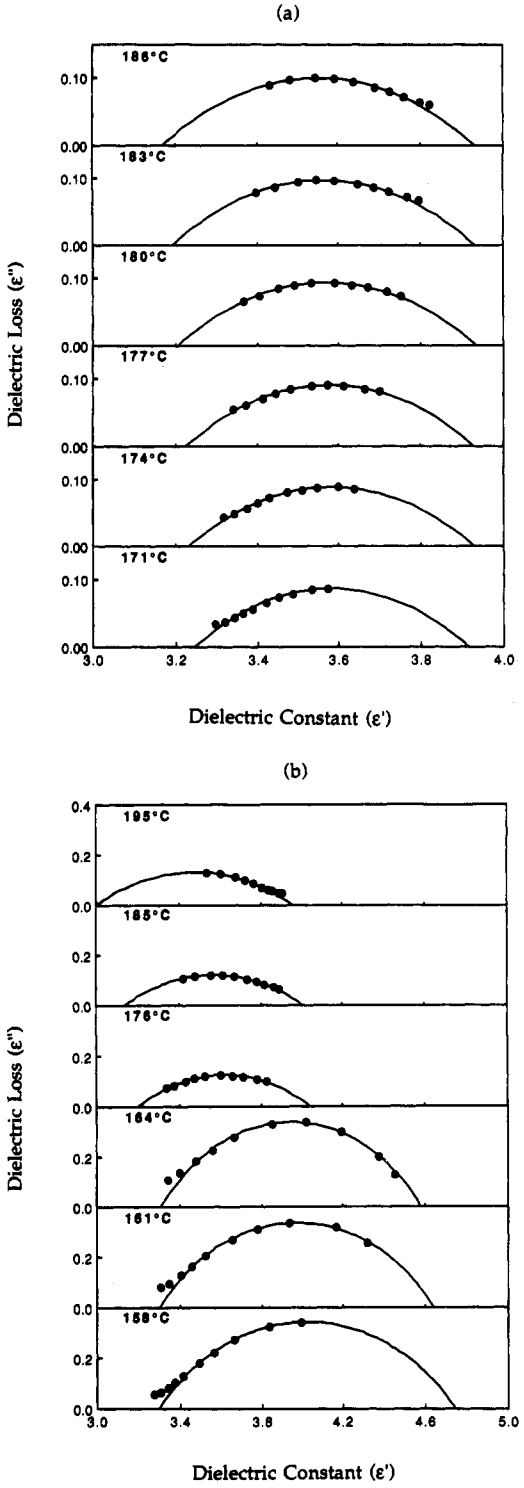

Figure 8. Cole–Cole plot, ϵ'' vs ϵ', at selected temperatures for (a) PEEK cold crystallized at $T_c = 200$ °C; (b) amorphous PEEK.

4.3. Dielectric Relaxation Intensity. Equation 1 was used to analyze the relaxation data for all PEEK samples shown in Table I. The ϵ'' vs ϵ' data for all semicrystalline PEEK samples were very symmetric, which is similar to what we observed in PPS.[16] Therefore, we assumed that $a_2 = 1$, and fit our data to a circle with the origin displaced below the $\epsilon'' = 0$ line, generating Cole–Cole plots.[48] Examples of Cole–Cole plots are shown in Figure 8, parts a and b, for one representative semicrystalline sample and the amorphous PEEK sample. Symbols represent the actual data points, and the line is the arc of the best fitting circle. On the right-hand side of the circle, we occasionally see evidence of ionic conductivity which increases the low frequency loss component (see Figure 8, part a, 186 °C, for example). For data close to the left-hand side of the circle, we see the beginning of another relaxation (sub-T_g), which causes the high frequency loss component to increase (see Figure 8, part b, 158 °C, for example).

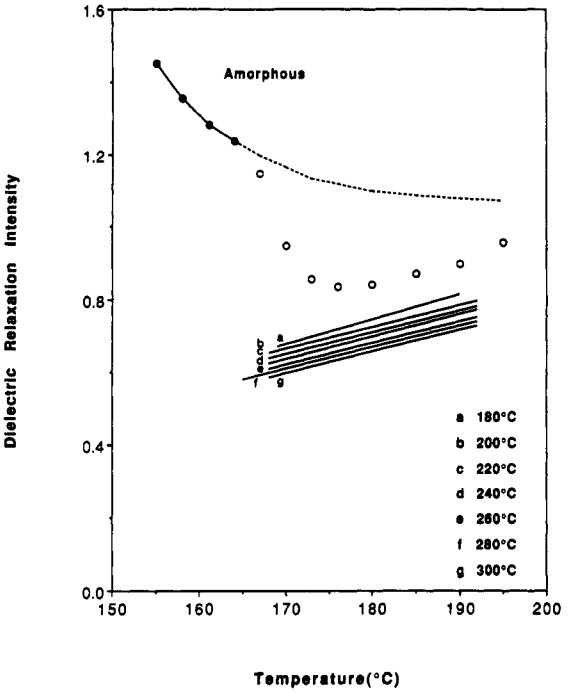

Figure 9. Dielectric relaxation intensity ($\Delta\epsilon$) as a function of temperature for PEEK cold crystallized at the temperatures indicated for a–g and for amorphous PEEK: (●) before crystallization; (○) after crystallization; (- - -) estimated dielectric intensity for noncrystallizable PEEK.

From the circle intersection with the ϵ' axis, we see the temperature dependence of the difference between the upper intersection (ϵ_s) and lower one (ϵ_∞). This is the dielectric relaxation intensity ($\Delta\epsilon$) defined by eq 2. For the semicrystalline relaxation, Figure 8, part a, as measurement temperature increases the relaxation intensity increases, and this result is characteristic of all the cold crystallized PEEK samples. In Figure 8, part b, the quenched PEEK is shown for a range of temperatures over which the sample crystallizes. For temperatures 158, 161, and 164 °C the material is still amorphous. The relaxation intensity, $\Delta\epsilon$, decreases in this temperature range. Above 164 °C, PEEK crystallizes rapidly and by 176 °C the relaxation intensity from the circle intersections is much smaller than that for the quenched material. Then, as temperature increases from 176 to 195 °C, the relaxation intensity increases.

The temperature dependence of the dielectric relaxation intensity, $\Delta\epsilon(T)$ vs T, is shown in Figure 9 for the amorphous and semicrystalline PEEK. The temperature dependence is different for the two types of samples. For all of the semicrystalline samples (shown by the solid lines), the relaxation intensity increases with increasing measurement temperature. In addition, the dielectric relaxation intensity is greater the lower the cold crystallization temperature of the PEEK. This can be readily intepreted by considering the T_c dependence of the degree of crystallinity from Table I. The semicrystalline PEEK has a smaller degree of crystallinity when cold crystallized at a lower temperature. Thus, there is a larger fraction of amorphous dipoles and the intensity of the relaxation is increased.

Relaxation intensity of amorphous PEEK decreases as the temperature increases before the crystallization takes place. This is shown by the solid symbols in Figure 9. The intensity then decreases quite sharply when the amorphous

sample becomes crystallized after 164 °C (open symbols). Relaxation intensity increases again, as the temperature increases further, in a way similar to that of the semicrystalline samples. The only difference is that the magnitude of the relaxation intensity is greater than that of the isothermally cold crystallized samples. This relaxation intensity is now that of the amorphous phase in the semicrystalline sample. Intensity is higher because of the larger amount of amorphous phase (80% determined by DSC), compared with all other cold crystallized samples.

The assumed temperature dependence of amorphous, noncrystallizable PEEK is shown by the dashed line in Figure 9. This represents our guess about the extrapolation of the 100% amorphous relaxation strength to higher temperatures. Generally, $\Delta\epsilon$ for the amorphous phase above T_g decreases as a consequence of increasing temperature[22] though there are several forms used to express the functional dependence. The theory developed by Onsager[49] predicts that the dielectric intensity is proportional to the reciprocal of the temperature. Kirkwood extended Onsager's result to account for autocorrelation of the dipoles.[50] According to Kirkwood, besides the $1/T$ dependence, there is another term which comes from cooperativity (autocorrelation) of the dipoles, and this term may also be temperature dependent. In fact, we observe a steeper than $1/T$ decrease in the dipolar relaxation of the amorphous PEEK. This indicates that the cooperative interaction decreases with an increase of temperature.[51]

The general decrease in dielectric relaxation intensity with increasing temperature has been also observed for other polymers such as PPS[16] and PET.[18] The physical reason behind this decrease can be described in the following way. For dielectric measurement above the glass transition temperature, the electric field and temperature have different effects on the orientation of dipoles. The thermal energy of the dipoles tends to randomize them, reducing their orientational polarizability. The electric field is no longer effective in dipole alignment, and the result of increasing temperature further above T_g is to randomize the dipoles more, causing a decrease in $\Delta\epsilon$.

For semicrystalline samples, this should also be true if all dipoles in the amorphous phase were to become relaxed. Based simply on the temperature dependence of the polarizability, we would expect relaxation strength at $T > T_g$ to decrease with increasing temperature. In fact we have observed this trend in other semicrystalline polymers such as New-TPI polyimide.[52] But this is not what we observe from the measurement of $\Delta\epsilon$ of the semicrystalline PEEK samples. The different behavior of $\Delta\epsilon(T)$ for semicrystalline samples compared to that of the 100% amorphous phase indicates that there is another factor controlling the temperature dependence of relaxation intensity. The factor is the additional relaxation of rigid amorphous phase dipoles.

$\beta(T)$, defined in eq 3, is the total amount of material relaxed at $T > T_g$. In fact, $\beta(T)$ is a better method than using $\gamma(T)$ for determining the mobile fraction because it has no reliance on the degree of crystallinity and does not suffer the same problem of base-line determination. $\beta(T)$ can be used in cases where the glass transition relaxation and the crystal relaxation are well separated, which is the situation for PEEK and PPS.[16] Evaluation of $\beta(T)$ would allow us to compare its numerical value to χ_a or $\gamma(T_g)$ calculated according to eq 5. As we see from Table I, the liquid-like amorphous phase shows a very weak dependence on the crystallization temperature, a result that agrees with previous studies.[15,16] However, the degree of crystallinity determined from DSC heat of fusion increases as T_c increases. This results in a decrease in RAP content as the crystallization temperature increases.

The parameter $\beta(T)$ can be estimated from the data presented in Figure 9, by extrapolating the amorphous intensity (prior to crystallization) and semicrystalline intensity to overlapping temperature regions. For the amorphous PEEK, it is impossible to measure the dielectric relaxation intensity at temperatures higher than 164 °C because of rapid crystallization. Therefore we use the extrapolated portion of the amorphous intensity (dashed line in Figure 9) to compute $\beta(T)$ for all semicrystalline samples. This will result in some uncertainty for the quantitative value of $\beta(T)$. But qualitatively it is certain the dielectric intensity of amorphous PEEK above T_g *decreases* as temperature increases,[22] and the dielectric intensity of semicrystalline samples *increases* as temperature increases.

This leads to two conclusions. First, $\beta(T)$ for all semicrystalline PEEK samples increases with increasing temperature and thus provides strong evidence that the fraction of relaxing units increases as the temperature of measurement increases. Second, in spite of possible error in estimating the numerical value of $\beta(T)$, the error, if it exists, is a systematic one. It will not change the sequence of the semicrystalline samples in Figure 9. This indicates that the lower the cold crystallization temperature, the more the total amorphous phase is relaxed above T_g. In other words, though there is nearly the same amount of mobile amorphous phase for all crystallization temperatures, the PEEK samples that relax the most (largest $\beta(T)$) are those with the largest amount of rigid amorphous-phase material.

One possible source which could contribute to $\beta(T)$ at high temperatures would be crystal premelting, in addition to the relaxation of the amorphous phase. In other words, the amount of amorphous-phase material may be increasing during the test. However, from our DSC data, these samples (with the exception of the one crystallized at T_c = 180 °C) do not show any discernable premelting up to the highest temperature we analyzed (192 °C) in Figure 9. For T_c = 180 °C, the highest measurement temperature, 192 °C, is very close to the first melting peak which occurs at about 195 °C. For all other PEEK samples, we conclude that no crystals melt up to 192 °C, and therefore the only contribution to $\beta(T)$ is from the mobile amorphous phase and rigid amorphous phase. No additional amorphous phase is created by crystal melting in this temperature range.

Here we have assumed that the crystal dipolar contribution (i.e., separate relaxation due to dipoles inside the crystals) is minimal at the temperatures over which our data are analyzed. This assumption is justified for the following reasons. First, from the raw data we see no evidence for an additional, or separate, high-temperature relaxation peak. The shape of the Cole–Cole plots is very symmetric, indicative of a single relaxation process. The slight upturn in the Cole–Cole plot at low frequency and high temperature is not included in the curve fitting for the determination of $\Delta\epsilon$. Second, any crystal dipole relaxation with a maximum at a temperature higher than that we tested will have negligible contribution to the temperature range below 200 °C. Further studies should be performed on melt-crystallized samples examined above 300 °C to locate the crystal dipole relaxation maximum.

The estimate of the numerical value of the $\beta(T)$ for semicrystalline samples allows us quantitatively to understand the relaxation and the temperature-dependent mobility of the interphase region of polymers such as PEEK. Based on the amorphous phase intensity extrapolation shown in Figure 9 (dashed line), our calculated value of $\beta(T)$ is 0.40–0.45 around 160 °C and 0.63–0.73 at about 192 °C, dependent on the different crystallization temperatures and

thus on the fraction of the rigid amorphous phase. These values are very consistent with our DSC results shown in Table I for the liquid-like amorphous phase (0.40) and total amount of amorphous phase (0.64–0.72).

Recalling the three different possible cases we proposed in section 2, we realize that PEEK, like PPS, is included in the second case, shown in Figure 1, curve 2. No rigid amorphous material relaxes below T_g. Only that portion of the liquid-like amorphous phase is relaxed which contributes to the heat capacity increment at T_g. For the cold-crystallized PEEK we studied, χ_a is about 0.40, irrespective of the cold crystallization temperature, as listed in Table I. This is also confirmed by our dielectric intensity measurement which shows the $\beta(T)$ at T_g is very close to 0.40. On the other hand, the upper limit of $\beta(T)$ (for $T < T_m$) should be the total fraction of amorphous phase, as we proposed in Figure 1.

Rigid amorphous-phase material is located at the boundary between the crystals and mobile amorphous phase. RAP then constitutes interphase chains whose dipoles are bound more tightly than the normal amorphous phase which becomes liquid-like at T_g and less tightly than dipoles in the crystalline regions. During cold crystallization at the lower crystallization temperatures, crystals form by dense nucleation from a state of very low chain mobility. We expect that the crystal/amorphous interphase chains may be highly entangled with the fold surface chains, contributing to the large amount of RAP at low T_c. As the crystallization temperature increases, the molecular mobility also increases. Chains are more likely to be able to disentangle during crystallization, relaxing stresses that occur during rapid nucleation. The interphase may be less restricted in this case, leading to a smaller amount of RAP.

5. Conclusions

Dielectric relaxation was used to explore the molecular mobility of PEEK containing a fraction of the rigid amorphous phase. We used the dielectric increment to determine the fraction of dipoles contributing to the large-scale segmental relaxation at temperatures above T_g. Our results show that the dielectric relaxation intensity is sensitive to the structure of the amorphous phase. PEEK contains both mobile amorphous and rigid amorphous chains which exhibit very different relaxation behavior: mobile amorphous chains relax over a narrow temperature range, indicative of a population of dipoles with a well-defined narrow relaxation time distribution. The rigid amorphous-phase dipoles, on the other hand, do not show a separate glass transition temperature but relax little by little as the temperature increases above the glass transition of the mobile amorphous phase. We have demonstrated for the first time that rigid amorphous-phase material in PEEK represents chains with a temperature-dependent mobility. In semicrystalline PEEK, the fraction of relaxing dipoles increases with temperatures above T_g.

Acknowledgment. This research was supported by NSF-MRL (DMR87-19217).

References and Notes

(1) Flory, P. J. *J. Am. Chem. Soc.* **1962**, *84*, 2857.
(2) Popli, R.; Mandelkern, R. *Polym. Bull.* **1983**, *9*, 260.
(3) Flory, P. J.; Yoon, D. Y.; Dill, K. A. *Macromolecules* **1984**, *16*, 862.
(4) Yoon, D. Y.; Flory, P. J. *Macromolecules* **1984**, *17*, 868.
(5) Popli, R.; Glotin, M.; Mandelkern, L.; Benson, R. S. *J. Polym. Sci.* **1984**, *22*, 407.
(6) Hahn, B.; Wendorff, J.; Yoon, D. J. *Macromolecules* **1985**, *18*, 718.
(7) Hahn, B.; Herrmann-Schonherr, O.; Wendorff, J. H. *Polymer* **1987**, *28*, 201.
(8) Loufakis, K.; Wunderlich, B. *Macromolecules* **1987**, *20*, 2474.
(9) Gaur, U.; Wunderlich, B. *J. Phys. Chem. Ref. Data* **1981**, *10*, 119.
(10) Wunderlich, B.; Czornyi, G. *Macromolecules* **1977**, *10*, 906.
(11) Lau, S.-F.; Wunderlich, B. *J. Polym. Sci., Polym. Phys. Ed.* **1984**, *22*, 379.
(12) Grebowicz, J.; Lau, S. F.; Wunderlich, B. *J. Polym. Sci., Polym. Symp.* **1984**, *71*, 19.
(13) Suzuki, H.; Grebowicz, J.; Wunderlich, B. *Makromol. Chem.* **1985**, *186*, 1109.
(14) Cheng, S. Z. D.; Wu, Z. Q.; Wunderlich, B. *Macromolecules* **1987**, *20*, 2802.
(15) Cheng, S. Z. D.; Cao, M. Y.; Wunderlich, B. *Macromolecules* **1986**, *19*, 1868.
(16) Huo, P.; Cebe, P. *J. Polym. Sci., Polym. Phys. Ed.*, in press.
(17) Huo, P.; Cebe, P. *Mater. Res. Soc. Symp. Proc.* **1991**, *215*, 93.
(18) Schlosser, E.; Schonhals, A. *Colloid Polym. Sci.* **1989**, *267*, 963.
(19) Schick, C.; Nedbal, J. *Progr. Colloid Polym. Sci.* **1988**, *78*, 9.
(20) Huo, P.; Cebe, P. *Colloid Polym. Sci.*, in press.
(21) Havriliak, S.; Negami, S. *Polymer* **1967**, *8*, 161.
(22) McCrum, N. G.; Read, B. E.; Williams, G. *Anelastic and Dielectric Effects in Polymeric Solids*; John Wiley and Sons: New York, 1967.
(23) Blundell, D. J.; Osborn, B. N. *Polymer* **1983**, *24*, 953.
(24) Yoda, O. *Polym. Commun.* **1984**, *25*, 238.
(25) Cebe, P. *J. Mater. Sci.* **1988**, *23*, 3721.
(26) Cebe, P.; Chung, S. Y.; Hong, S. *J. Appl. Polym. Sci.* **1987**, *33*, 487.
(27) Ashcraft, C. R.; Boyd, R. H. *J. Polym. Sci., Polym. Phys. Ed.* **1976**, *14*, 2153.
(28) Goodwin, A. A.; Hay, J. N. *Polym. Commun.* **1989**, *30*, 222.
(29) D'Amore, A.; Kenny, J. M.; Nicolais, L. *Polym. Eng. Sci.* **1990**, *30*, 314.
(30) Starkweather, H. W. Jr.; Avakian, P. *Macromolecules* **1989**, *22*, 4060.
(31) Sasuga, T.; Hagiwara, M. *Polymer* **1985**, *26*, 501.
(32) Sasuga, T.; Hagiwara, M. *Polymer* **1986**, *27*, 821.
(33) Sasuga, T.; Hagiwara, M. *Polymer* **1987**, *28*, 1915.
(34) Thompson, S. A.; Farris, R. J. *J. Appl. Polym. Sci.* **1988**, *36*, 1113.
(35) Chan, C. M.; Venkatraman, S. *J. Polym. Sci., Polym. Phys. Ed.* **1987**, *25*, 1655.
(36) Stober, E. J.; Seferis, J. C. *Polymer* **1984**, *25*, 1845.
(37) Coburn, J. C.; Boyd, R. H. *Macromolecules* **1986**, *19*, 2238.
(38) Cebe, P.; Hong, S. *Polymer* **1986**, *27*, 1183.
(39) Nguyen, H. X.; Ishida, H. *Polymer* **1986**, *27*, 1400.
(40) Nguyen, H. X.; Ishida, H. *J. Polym. Sci., Polym. Phys. Ed.* **1986**, *24*, 1079.
(41) Blundell, D. J. *Polymer* **1987**, *28*, 2248.
(42) Lee, Y.; Porter, R. S. *Macromolecules* **1988**, *20*, 1336.
(43) Chang, S. *Polym. Commun.* **1989**, *29*, 139.
(44) Bassett, D. C.; Olley, R. H.; Al Raheil, I. A. M. *Polymer* **1988**, *29*, 1745.
(45) Lee, Y.; Porter, R. S. *Macromolecules* **1988**, *20*, 2770.
(46) Lee, Y.; Porter, R. S. *Macromolecules* **1989**, *21*, 1756.
(47) Donth, E. *J. Non-Cryst. Solids* **1982**, *53*, 325.
(48) Cole, R. H.; Cole, K. S. *J. Chem. Phys.* **1941**, *9*, 341.
(49) Onsager, L. *J. Am. Chem. Soc.* **1936**, *58*, 1486.
(50) Kirkwood, J. G. *J. Chem. Phys.* **1939**, *7*, 911.
(51) Zou, D.; Iwasaki, S.; Tsutsui, T.; Saito, S. *Polymer* **1990**, *31*, 1888.
(52) Huo, P.; Cebe, P. *Mater. Res. Soc. Symp. J.* Anaheim, CA, April, 1991.

Registry No. PEEK, 31694-16-3.